

HIDDEN SYMMETRY CONCEPTS IN THE ELASTIC BUCKLING OF AXIALLY-LOADED CYLINDERS

G. W. HUNT, K. A. J. WILLIAMS† and R. G. COWELL‡

Department of Civil Engineering, Imperial College London, London SW7 2BU, U.K.

(Received 10 May 1985; in revised form 20 December 1985)

Abstract—The recognized harmonic buckling modes for the elastic axially-loaded cylinder are by nature symmetric, equal and opposite amplitudes giving equal energy levels. On the other hand, in combination they account for considerable asymmetry, inwards deflection being fundamentally different from outwards; this asymmetry is also apparent in the underlying differential equations, and in the final large-deflection Yoshimura pattern. Taking the view that underlying symmetries are closely linked to the form of bifurcation experienced on buckling, and hence to the gross instability of the phenomenon, the paper thus explores a classic problem in a new light. The well-known Donnell equations are first employed, the analysis being neatly written in terms of the two variables radial displacement w and stress function Φ . An extension is then presented, derived from the full strain–displacement equations appropriate to genuinely large deflections. This makes use of a suite of computer programs, written for a small micro, which handle the required manipulations of multiplication and integration of harmonic functions in algebraic rather than numerical fashion.

1. INTRODUCTION

The thin cylinder under axial load is one of the classic bifurcation problems of elastic structures. The importance in design, the inherent complexity, and the severe instability, combine to give it a special significance. It has been the subject of innumerable different theoretical approaches, yet significant questions remain[1]. Under such circumstances it seems sensible to extend the range of interest beyond just that of mechanics, taking into account, where possible, recent developments in applied mathematics. To some extent this is the aim here. A new computerized analytical scheme is also introduced based on general stability theory[2, 3], working from the full, as well as the better-known Donnell, membrane strain–displacement relations. In the present work the effects of imperfections are ignored, although the close link between the bifurcational response of a perfect system and imperfection-sensitivity provides a clear way forward.

The historical developments are well known. The early paper of Donnell[4] was the first to draw attention to the important interactive effects which are so closely associated with the extreme instability of the axially-loaded cylinder. von Kármán and Tsien[5] were also instrumental in exploring the nature of the instability; in focusing on shell curvature, their work leads naturally to an examination of the different roles played by quadratic, cubic and quartic terms of energy. The next significant step came from Koiter[6], who saw the problem in the modern bifurcational context, introducing the concept of imperfection-sensitivity by exploring initial perturbations from an ideal state; this anticipated the later development of “universal unfolding”[7]. The approach initiated by Donnell continued with later investigators adding increasingly more harmonic modes to the Rayleigh–Ritz description for w [8, 9]. This finished up with Hoff *et al.*[10] who effectively demolished the search for the “minimum post-buckling load” by showing that the predicted minimum load approached zero with decreasing shell thickness.

Meanwhile a number of workers have contributed significantly in other ways. Croll[11] associates the destabilization and subsequent restabilization of cubic and quartic energy terms with a particular (stabilizing) quadratic term, and thus gets results from a linear eigenvalue study that compare well with experiment. Alternatively, Calladine[1] draws this

† Present address: J. P. Kenny & Partners, 88–89 High Holborn, London WC1V 6LS, U.K.

‡ Present address: School of Mathematical Sciences, Queen Mary College, London E1 4NS, U.K.

complex nonlinear problem into his general framework for shells, pin-pointing the same modal interactions that we find from symmetry considerations below. Much work has been done on the effects of imperfections. Koiter's second important contribution was to feed an imperfection into an axi-symmetric buckling mode, studying the bifurcations into the non-symmetric modes thus produced[12]; this provided more realistic predictions of failure loads for imperfections of finite size than earlier asymptotic approaches. Hansen[13] extended Koiter's classic formulation[6] to five separate imperfection forms. More practically, interest has recently centered on the development of international imperfection data banks, built from careful experimental study world-wide (see [14] for example). We note also the theoretical and experimental work conducted by the Centres for Marine Technology at London and elsewhere (see [15, 16] for example). A glance at the proceedings of the latest IUTAM Symposium on structural collapse gives an indication of the significance of the cylindrical form to both theory and practice[17].

Here our system is as idealized as possible, being an infinitely long, thin cylindrical shell, imperfection free, restrained against overall buckling as a column. We concentrate on the initial post-buckling, examining bifurcations from the linear fundamental equilibrium path which represents pure squash and dilation. The classical buckling modes are axi-symmetric and non-symmetric harmonic functions, and interest focusses on a pivotal interaction between two typical modes, one axi-symmetric and the other non-symmetric; this is seen to have a strong symmetry-breaking effect on the topological form of the underlying potential energy function. The need to consider boundary conditions at the ends of the cylinder, which become more significant as the length decreases, is avoided; this complicates the issue by making the fundamental path nonlinear, and obscures the interesting topology of the interaction.

Briefly, the argument is as follows[18]. Cylinder buckling, when measured in terms of radial displacement w , carries an underlying asymmetry, inwards being fundamentally different from outwards. But each of the buckling modes is symmetric in its own right, being harmonic both axially and circumferentially; equal and opposite amplitudes give identical energy levels. The only possible exception for a finite length shell is an axi-symmetric mode, and if this should have an even number of longitudinal half-waves (the limiting case as length approaches infinity) then it also is symmetric, guaranteed by symmetry about the half-length. It is only by combining that the modes can satisfy the required asymmetry, and this coupled with the fact that they can have the same or similar critical loads makes mode interaction inevitable. It should be noted that the final deformed shape, the well-known Yoshimura or diamond pattern, is profoundly asymmetric, being circumferentially polygonal and impossible to reverse.

Modern applied mathematics has only recently recognized the importance of symmetries which appear in the modes but not in the final deformed shape and thus not in the underlying governing differential equation[18, 19]. These are referred to as "hidden" and "subtle" symmetries since, in the interests of rigour, mathematicians are more likely to treat problems as continuous than discrete. Their presence can, however, radically alter the classification of the initial buckling phenomenon, and it is clear that the deeper understanding comes from considering the modes both separately and in combination. It is also the case that, in many well-known structural examples, it is not the modal symmetries but the underlying asymmetry that is less immediately obvious; we see this in the Shanley model[20].

Perturbation analysis based on such symmetry properties turns out to be quite different in character from conventional procedures[21], as we show here for the cylinder problem using Rayleigh-Ritz modelling. To carry this out efficiently, a suite of reduction programs has been written in Pascal and implemented on a microcomputer. The scheme employs codified integer variables rather than real numbers to maintain 100% accuracy. Routines are developed to determine systematically the u and v forms for an input w , differentiate appropriately for the strains, and multiply and integrate for the total energy, which is then output as a stream of integer numbers. Operating on this, the general theory of elastic stability[2] together with the new procedures[3] then gives equilibrium paths which are directly plotted. The analytical scheme is readily adaptable to other structural problems.

2. FORMULATION

A very general treatment for the classical nonlinear buckling of the (infinitely long) cylinder under axial load can be initiated by substituting the following expansions for radial, longitudinal and tangential displacement,

$$\begin{aligned}
 w &= Q_0 R + q_1 l \cos \frac{ny}{R} \cos \frac{\pi x}{2l} + q_2 l \cos \frac{\pi x}{l} + q_3 l \cos \frac{2ny}{R} + q_4 l \cos \frac{ny}{R} \cos \frac{3\pi x}{2l} \\
 &\quad + q_5 l \cos \frac{3ny}{R} \cos \frac{\pi x}{2l} + q_6 l \cos \frac{2ny}{R} \cos \frac{\pi x}{l} + q_7 l \cos \frac{2\pi x}{l} + q_8 \cos \frac{4ny}{R} + \dots, \\
 u &= B_0 x + b_1 l \cos \frac{ny}{R} \sin \frac{\pi x}{2l} + b_2 l \sin \frac{\pi x}{l} + b_4 l \cos \frac{ny}{R} \sin \frac{3\pi x}{2l} \\
 &\quad + b_5 l \cos \frac{3ny}{R} \sin \frac{\pi x}{2l} + b_6 l \cos \frac{2ny}{R} \sin \frac{\pi x}{l} + b_7 l \sin \frac{2\pi x}{l} + \dots, \quad (1) \\
 v &= c_1 l \sin \frac{ny}{R} \cos \frac{\pi x}{2l} + c_3 l \sin \frac{2ny}{R} + c_4 l \sin \frac{ny}{R} \cos \frac{3\pi x}{2l} \\
 &\quad + c_5 l \sin \frac{3ny}{R} \cos \frac{\pi x}{2l} + c_6 l \sin \frac{2ny}{R} \cos \frac{\pi x}{l} + c_8 l \sin \frac{4ny}{R} + \dots,
 \end{aligned}$$

into the full strain–displacement relations on the middle-surface of the thin elastic cylinder [6, 10, 22],

$$\begin{aligned}
 \varepsilon_x &= \frac{\partial u}{\partial x} + \frac{1}{2} \left(\frac{\partial w}{\partial x} \right)^2 + \frac{1}{2} \left(\frac{\partial u}{\partial x} \right)^2 + \frac{1}{2} \left(\frac{\partial v}{\partial x} \right)^2, \\
 \varepsilon_y &= \frac{\partial v}{\partial y} + \frac{w}{R} + \frac{1}{2} \left(\frac{\partial w}{\partial y} - \frac{v}{R} \right)^2 + \frac{1}{2} \left(\frac{\partial v}{\partial y} + \frac{w}{R} \right)^2 + \frac{1}{2} \left(\frac{\partial u}{\partial y} \right)^2, \quad (2) \\
 \varepsilon_{xy} &= \frac{\partial v}{\partial x} + \frac{\partial u}{\partial y} + \frac{\partial w}{\partial x} \left(\frac{\partial w}{\partial y} - \frac{v}{R} \right) + \frac{\partial v}{\partial x} \left(\frac{\partial v}{\partial y} + \frac{w}{R} \right) + \frac{\partial u}{\partial x} \frac{\partial u}{\partial y},
 \end{aligned}$$

where $2l$ is the sample length of the cylinder (one half-wave longitudinally in q_1) and R is the radius. We note that these equations are developed from the definition of strain as $(1/2) \times [\text{change in (length)}^2] / (\text{original length})^2$ [22], rather than the more usual, change in length/original length. As the value of strain approaches zero the two definitions coincide, so the former can be taken for the small strains of interest here; it leads to considerable reduction in complexity, Pythagorean square roots being eliminated, and makes the development of extended equations at least possible. An alternative, although they may miss certain relevant quartic energy terms, is to take the familiar reduced strain–displacement relations attributed to Donnell [4],

$$\begin{aligned}
 \varepsilon_x &= \frac{\partial u}{\partial x} + \frac{1}{2} \left(\frac{\partial w}{\partial x} \right)^2, \\
 \varepsilon_y &= \frac{\partial v}{\partial y} + \frac{w}{R} + \frac{1}{2} \left(\frac{\partial w}{\partial y} \right)^2, \quad (3) \\
 \varepsilon_{xy} &= \frac{\partial v}{\partial x} + \frac{\partial u}{\partial y} + \frac{\partial w}{\partial x} \frac{\partial w}{\partial y}.
 \end{aligned}$$

These are substituted into the standard strain energy of stretching expression[23],

$$W_S = \frac{Et}{2(1-\nu^2)} \int_0^{2l} \int_0^{2\pi R} \left(\varepsilon_x^2 + \varepsilon_y^2 + 2\nu\varepsilon_x\varepsilon_y + \frac{(1-\nu)}{2} \varepsilon_{xy}^2 \right) dx dy, \quad (4)$$

to give the membrane energy in terms of the generalized coordinates q_i , b_i and c_i . We note that, substituting into the standard bending energy expression,

$$W_B = \frac{Et^3}{24(1-\nu^2)} \int_0^{2l} \int_0^{2\pi R} \left\{ \left(\frac{\partial^2 w}{\partial x^2} + \frac{\partial^2 w}{\partial y^2} \right)^2 - 2(1-\nu) \left[\frac{\partial^2 w}{\partial x^2} \frac{\partial^2 w}{\partial y^2} - \left(\frac{\partial^2 w}{\partial x \partial y} \right)^2 \right] \right\} dx dy, \quad (5)$$

generates only quadratic energy terms. It is thus clear that the profoundly nonlinear effects of cylinder buckling are due to the rapidly adjusting membrane state in the neutral surface of the shell. The work done by the axial load P is simply,

$$W_L = P \int_0^{2l} \frac{\partial u}{\partial x} dx = 2PlB_0 \quad (6)$$

and the total potential energy of the system (structure plus load) is given by,

$$V = W_S + W_B - W_L. \quad (7)$$

Compared with the extended formulation, the use of the Donnell equations means considerable savings in analytical effort. It is well known that, for the reduced form of eqns (3), the u and v displacements can neatly be replaced by a corresponding stress function, which appears linearly in the associated compatibility equation and thus can be eliminated completely; the problem is then quickly reduced to one in w alone. An alternative is to eliminate the u and v contributions as passive coordinates[2, 24], which involves greater analytical effort but is applicable also (in an asymptotic sense) to the extended equations. We shall see both reductions later.

Analysis proceeds as follows. First the fundamental path representing the pure dilation, $Q_0^F(P)$, and compression, $B_0^F(P)$, of the cylinder is removed by using incremental coordinates q_0 and b_0 measured from the path and defined by,

$$Q_0 = Q_0^F(P) + q_0, \quad B_0 = B_0^F(P) + b_0, \quad (8)$$

P being the applied load. We note that, should the full formulation of (2) be adopted, the fundamental path turns out to be mildly nonlinear. This effect is introduced by the unusual definition of strain discussed above, and for the small strains relevant here is slight and can be ignored.

Before the elimination of the u and v contributions, either by stress function or passive coordinates, the potential function V is non-diagonalized, a direct result of the w/R term in ε_y of the strain-displacement relations; quadratic cross terms of energy thus exist. However, the non-diagonalization is of a banded form, these cross terms occurring only when the suffixes of the q_i , b_i or c_i coordinates match, so,

$$V_{ij}^F = 0 \quad \text{for } i \neq j, \quad (9)$$

subscripts being used to denote indiscriminate partial differentiation with respect to either q_i , b_i or c_i , unlike the earlier fuller notation[2, 24, 25]; superscript F , as before, denotes evaluation on the fundamental path. We note that extra flags need to be carried in a more detailed analysis to distinguish between u , v or w contributions[26]. The non-diagonalization leads to the general condition for the non-critical fundamental state,

$$V_{ii}^F \neq 0. \quad (10)$$

This implies that, unlike in a corresponding plate analysis, the u and v deflections take a first-order significance, which in turn suggests that quartic energy terms are missing from the simplified Donnell approach, when deflections of the order necessary to determine the minimum post-buckling load are present; this can be seen from the form of the non-diagonalized elimination of passive coordinates equations[2], and was of course recognized by Hoff *et al.*[10]. The effect is examined in Section 5.

The elimination of the u and v components is described in both stress function (Section 4) and elimination of passive coordinates (Section 5) terms, beginning with the Donnell equations and full equations respectively. Subsequent elimination of the incremental dilation q_0 as a passive effect is also similarly achieved. However the remaining q_i are more of a problem, as discussed later in Section 6. Not only are there a large number of coincident, and near-coincident, contributing modes at the lowest critical point on the fundamental path[6], but eliminating q_3 as a passive effect is prone to severe convergence problems[26], even though this inextensional mode has no axial load term associated with it and thus has an infinite critical load. It is at this stage that it is rewarding to examine the symmetry properties of the reduced potential function $A(q_i, P)$, i varying between 1 and n , which we note is by now diagonalized so q_i represents the buckling modes. Coefficients of a Taylor expansion about F are determined by either reduction process, up to and including quartic terms; for the simplified Donnell formulation the function is truncated at this level, but under the full formulation it has a tail of higher-order terms.

3. SYMMETRIES

The concepts of symmetry and symmetry-breaking are now seen as being of fundamental significance in the classification of phenomena (see, for example, Sattinger[27]), and can be used with good effect to find and focus attention on the important interactive effects of the early post-buckling regime. We shall here use the concept of “flip invariance”[19], associated with the question “does the system take up the same shape, and hence have the same energy, when modes are reversed to equal and opposite amplitudes?” This complements analysis, by identifying certain modal interactions with significant non-zero cubic terms, that can then be found directly. We note that symmetry in a mode or combination of modes is a sufficient but not a necessary condition for elimination of an associated cubic; sometimes a term may be absent although an apparently relevant symmetry condition is not satisfied. However by and large the concept is useful, and significantly reduces the complexity of the initial formulation.

We see that each of the modes represented by the w form of eqn (1) is flip invariant if considered alone. The top of Fig. 1 shows a portion of circumferential section, at a constant x value, with $\xi = ny/R$ say. Clearly, for any chequerboard mode q_1 , the same deflection pattern is produced for negative as for positive amplitude, as shown. The fact that this is true at every section means that the system carries a fundamental symmetry in q_1 alone, and rules out terms in q_1^3 in the final potential function[2, 24]. The same holds for the axially-constant “rosette” mode q_3 , while the axi-symmetric mode q_2 is flip invariant under the proviso that it carries an even number of half waves longitudinally. Thus no single mode alone represents a good Rayleigh–Ritz approximation, since none accommodates the fundamental underlying asymmetry.

The second and third diagrams of Fig. 1 show the two different symmetry circumstances that can arise when two modes combine. If a cosine function is added to a cosine harmonic of odd degree, as shown in the second diagram, then the inwards deflection pattern over the range $\pi/2$ to $3\pi/2$ is repeated outwards over the range $3\pi/2$ to $5\pi/2$. The combination is then flip invariant, since the same pattern is repeated when both modes are simultaneously reversed. This means that, although shell geometry dictates that inwards deformation is fundamentally different from outwards, this particular combination of modes cannot accommodate the asymmetry. It also means that cross-term cubic energy contributions from the two modes vanish[2, 24]. We note that the same property of flip invariance is found for a cosine function combining with both odd and even sine harmonics, although these interactions are not specifically illustrated.

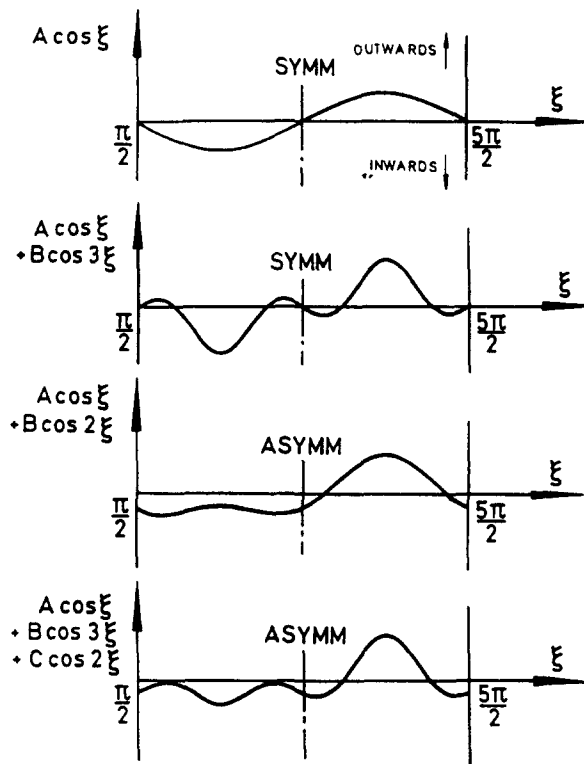


Fig. 1. Symmetry properties of modal combinations.

But if the cosine function is added to a cosine harmonic of even degree, as shown in the third diagram, the combination allows the asymmetry. We see that inwards deflection is now quite different from outwards, so reversing the modes does not necessarily give the same energy level. Modes which bear this relation to one another can thus interact profoundly at the cubic level. Considering modes q_1 and q_2 of eqn (1) for instance, the deflection pattern of the third diagram is found for every section of constant y ; here ξ can be taken as $\pi x/2l$. Regardless of the sign of the longer wavelength amplitude, the steeper-sided portion which is shown on the right-hand side remains pointing upwards (or outwards), while the flatter form of the left-hand side remains inwards; this can be seen as a good first approximation to the polygonal section of the well-known Yoshimura pattern. The asymmetry leads directly to the significant cubic A_{112}^F cross-term, and its counterpart in the circumferential direction to the corresponding term A_{113}^F , involving q_1 and q_3 .

The final diagram of Fig. 1 shows three modes together. Here the symmetric combination of the second diagram interacts with an even cosine harmonic in much the same way as previously, and asymmetry results. There is thus a significant three-fold interaction between q_1 , q_3 and q_5 of eqn (1), and an axial counterpart between q_1 , q_2 and q_4 . The appearance of cross-term cubics involving three modes at the lowest critical point [6] suggests that there are many different three-fold interactions which allow the asymmetry. It appears that, when three modes mix, asymmetry is the rule rather than the exception. This reinforces the point that multi-mode interaction is an inherent and inescapable part of cylinder buckling.

The interactive symmetry-breaking effect occurs between any (square or rectangular) chequerboard mode and its axi-symmetric (or rosette) counterpart, even though critical loads may not match. The modes having the lowest critical loads are those on the well-known Koiter half-circle of Fig. 2; this also shows the relation between the wavelengths of q_1 and q_2 , and their positions on the circle. It should be noted that the Koiter circle modes, although clearly relevant to initial post-buckling of the perfect system, may be superseded by others when imperfections are present; the general circle or ellipse in the space of Fig.

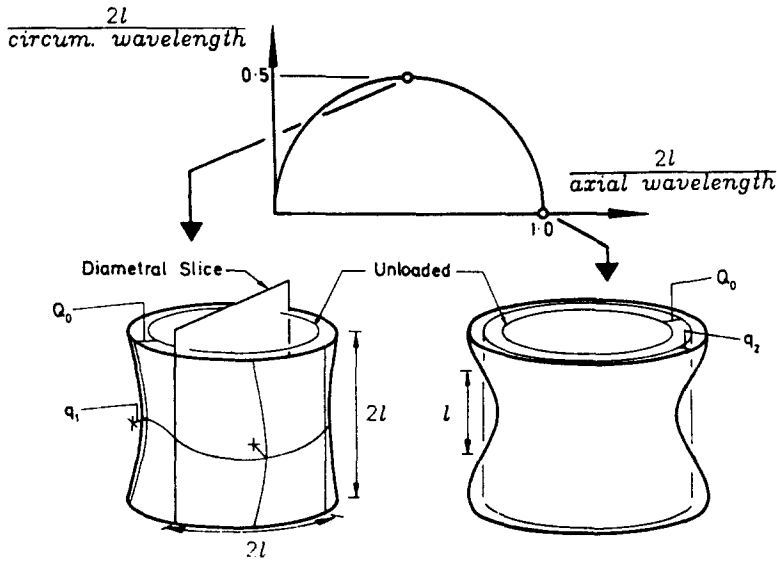


Fig. 2. The Koiter circle, and one well-known related modal interaction.

2 carries the same symmetries and associated energy terms as the Koiter circle, the only difference being that critical loads are not necessarily the same. Figure 3 shows the modes suggested by the asymmetry, those of eqn (1), in the wavelength-related space of Fig. 2, the Koiter circle being shown as an unbroken line and its circumferential counterpart as a broken line.

4. DONNELL EQUATIONS

The use of the Airy stress function with the simplified Donnell strain-displacement relations results in considerable economy of analysis, reducing the number of dependent variables from three to two. As we shall show, by restricting attention to harmonic variations in the stress function (apart from a term representing the applied stress), further simplifications are also made possible. We shall first consider a general radial displacement function w , discussing the relative importance of the various terms, before restricting attention to a three mode form for w , which is exactly solvable within the restrictions of the truncated (Rayleigh-Ritz) framework.

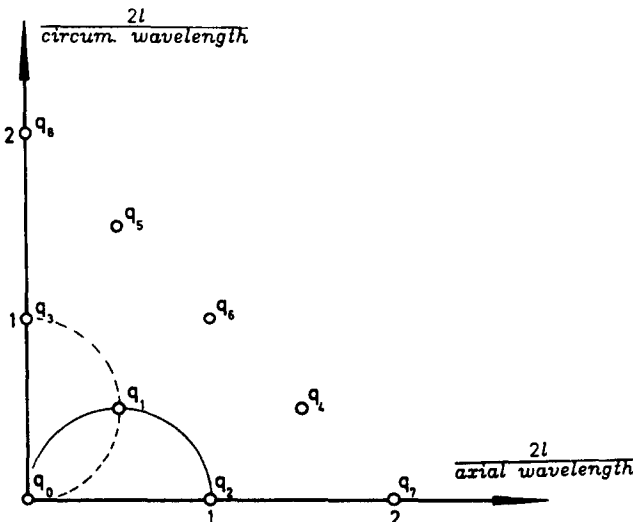


Fig. 3. The modes of eqn (1) in relation to the Koiter circle.

(a) *General analysis*

Full details for the introduction of the stress function, for orthotropic cylindrical shells with imperfections, can be found in the review article by Thielemann[28]; here we briefly outline the derivation for the perfect isotropic shell. Introducing the in-plane stress resultants,

$$N_x = \frac{Et}{1-\nu^2}(\varepsilon_x + \nu\varepsilon_y), \quad N_y = \frac{Et}{1-\nu^2}(\varepsilon_y + \nu\varepsilon_x), \quad N_{xy} = \frac{Et}{2(1+\nu)}\varepsilon_{xy}, \quad (11)$$

we define the stress function Φ in the usual way,

$$N_x = Et \frac{\partial^2 \Phi}{\partial y^2}, \quad N_y = Et \frac{\partial^2 \Phi}{\partial x^2}, \quad N_{xy} = -Et \frac{\partial^2 \Phi}{\partial x \partial y}. \quad (12)$$

These identically satisfy the well-known in-plane equilibrium equations,

$$\frac{\partial N_x}{\partial x} + \frac{\partial N_{xy}}{\partial y} = 0, \quad \frac{\partial N_{xy}}{\partial x} + \frac{\partial N_y}{\partial y} = 0. \quad (13)$$

Substituting the Donnell strain-displacement relations (3) into (11) and differentiating appropriately, the following compatibility equation arises,

$$\nabla^4 \Phi = \frac{1}{R} \frac{\partial^2 w}{\partial x^2} - \left[\frac{\partial^2 w}{\partial x^2} \frac{\partial^2 w}{\partial y^2} - \left(\frac{\partial^2 w}{\partial x \partial y} \right)^2 \right]. \quad (14)$$

On the other hand, employing the calculus of variations with respect to w on the total potential energy (7) yields the following equilibrium equation,

$$\frac{t^2}{12(1-\nu^2)} \nabla^4 w = -\frac{1}{R} \frac{\partial^2 \Phi}{\partial x^2} + \left(\frac{\partial^2 \Phi}{\partial x^2} \frac{\partial^2 w}{\partial y^2} + \frac{\partial^2 \Phi}{\partial y^2} \frac{\partial^2 w}{\partial x^2} - 2 \frac{\partial^2 \Phi}{\partial x \partial y} \frac{\partial^2 w}{\partial x \partial y} \right). \quad (15)$$

We see that u and v have now been entirely replaced by Φ .

Koiter[12] has discussed the significant differences between these two equations. Because of the linearity in Φ , the compatibility equation can symbolically be inverted, and the subsequent equation solved for Φ in terms of w . From eqn (14) we see that this solution has two additive contributions. The first comes from the linear term in w , and we denote it by,

$$\Phi^1 = \frac{1}{R} \nabla^{-4} \frac{\partial^2 w}{\partial x^2}. \quad (16)$$

This is a highly significant term, arising from the initial curvature of the cylinder; it is responsible both for raising the critical load above the flat plate (zero curvature) limit, and in interaction with the terms below, for the extreme instability at the critical point. The second contribution comes from the quadratic terms in w ,

$$\Phi^2 = -\nabla^{-4} \left[\frac{\partial^2 w}{\partial x^2} \frac{\partial^2 w}{\partial y^2} - \left(\frac{\partial^2 w}{\partial x \partial y} \right)^2 \right]. \quad (17)$$

This restabilizes the cylinder at moderately large deflections, but also interacts with the

linear contribution to generate destabilizing cubic terms of energy, as is further discussed below.

Consider a general periodic deflection in w of the form,

$$w = Q_0 R + \omega_{mn} \cos \frac{m\pi x}{2l} \cos \frac{ny}{R}, \tag{18}$$

where the first term is the pure dilation Poisson’s ratio effect, and the second term, employing Einstein’s convention, is a summation over all $m, n \geq 0$, but excluding $m = n = 0$. We see that the ω_{mn} have replaced the q_i of the general theory representation of eqn (1). The solution to eqn (16) is then simply,

$$\Phi^1 = -\frac{\Lambda y^2}{2} + \frac{\phi_{mn}^1}{R} \cos \frac{m\pi x}{2l} \cos \frac{ny}{R}, \quad \text{where } \phi_{mn}^1 = -\omega_{mn} \frac{\left(\frac{m\pi}{2l}\right)^2}{\left[\left(\frac{m\pi}{2l}\right)^2 + \left(\frac{n}{R}\right)^2\right]^2}. \tag{19}$$

Here the leading term represents the non-periodic applied stress, where $\Lambda = P/Et$, and on its own defines the fundamental equilibrium solution; its sole contribution is to the work done by the load, W_L . Clearly the amplitudes ϕ_{mn}^1 are linearly proportional to the corresponding ω_{mn} amplitudes. In similar manner, Φ^2 may be cast in terms of the w modes; to do so requires that products of cosines be reduced to sums of cosines. This is a straightforward procedure, and the result we summarize as,

$$\Phi^2 = \phi_{mn}^2 \cos \frac{m\pi x}{2l} \cos \frac{ny}{R}, \tag{20}$$

where the ϕ_{mn}^2 are quadratic functions of the ω_{mn} .

Rewriting the membrane energy in terms of the stress function, integrating by parts, and employing the fact that we use only periodic variations in w , we find that W_s can be reduced to the simple form,

$$W_s = \frac{Et}{2} \int_0^{2l} \int_0^{2\pi R} (\nabla^2 \Phi)^2 \, dx \, dy. \tag{21}$$

A similar reduction may be used for the bending energy, to give,

$$W_B = \frac{Et^3}{24(1-\nu^2)} \int_0^{2l} \int_0^{2\pi R} (\nabla^2 w)^2 \, dx \, dy, \tag{22}$$

while the potential energy of the load can be written,

$$W_L = \frac{\Lambda Et}{2} \int_0^{2l} \int_0^{2\pi R} \left(\frac{\partial w}{\partial x}\right)^2 \, dx \, dy. \tag{23}$$

With the aid of eqns (17)–(23), the contributions to the energy can be discussed in a straightforward manner. We employ the orthogonality properties of harmonic functions, and introduce the matrix function g_{mn} , defined by

$$g_{00} = 4; \quad g_{m0} = g_{0m} = 2 \quad \text{for } m > 0; \quad g_{mn} = 1 \quad \text{for } m > 0 \text{ and } n > 0. \tag{24}$$

After dividing by a factor of $Et/2$, the total potential energy can then be written,

$$V = W_S + W_B - W_L$$

$$= \left\{ \left[\left(\frac{\phi_{mn}^1}{R} + \phi_{mn}^2 \right)^2 + \frac{l^2}{12(1-\nu^2)} \omega_{mn}^2 \right] \left[\left(\frac{m\pi}{2l} \right)^2 + \left(\frac{n}{R} \right)^2 \right]^2 - \Lambda \left(\frac{m\pi}{2l} \right)^2 \omega_{mn}^2 \right\} g_{mn}, \quad (25)$$

where the summation convention is again employed over m and n .

We recall that the ϕ_{mn}^1 and ϕ_{mn}^2 are respectively linear and quadratic in the modal amplitudes of w . Thus the bending energy contributes stabilizing positive quadratic energy terms, while the work done by the load contributes destabilizing negative quadratic terms and is responsible for the presence of the bifurcation. The stretching energy has three separate effects as follows. The ϕ_{mn}^1 contribution alone gives rise to stabilizing positive quadratic terms, the amount of stabilization increasing with cylinder curvature and disappearing in the flat plate limit. Similarly, ϕ_{mn}^2 generates positive quartic terms, which stabilize the cylinder for moderately large deflections. What initiates the highly unstable behaviour at the critical load is the interactive cross-product between ϕ_{mn}^1 and ϕ_{mn}^2 , which yields cubic terms in the mode amplitudes ω_{mn} . The amount of destabilization is proportional to the cylinder curvature, again disappearing in the flat plate limit. Thus we have two opposing tendencies coming from the initial curvature, one a stabilizing influence on the quadratic terms, increasing the critical load and proportional to (curvature)², and the second a highly destabilizing set of cubic terms proportional to the curvature. In the flat plate limit both effects disappear, and we are left with the stable post-buckling behaviour associated with quadratic and quartic energy terms.

(b) *Three mode analysis*

Having discussed the general framework of the Donnell strain–displacement relations, we now present a three mode Rayleigh–Ritz analysis, employing the stress function. Specifically, for the reasons described in the earlier section on symmetries, we choose the following form for w ,

$$w = Q_0 R + q_1 l \cos \frac{\pi x}{2l} \cos \frac{ny}{R} + q_2 l \cos \frac{\pi x}{l} + q_3 l \cos \frac{2ny}{R}, \quad (26)$$

which is truncated after the first three terms of eqn (1). As outlined above, we can determine the associated stress function,

$$\Phi = -\frac{\Lambda y^2}{2} - \left[\frac{q_1 l}{R} + 2q_1(q_2 + q_3) \left(\frac{nl}{R} \right)^2 \right] \left\{ \frac{\left(\frac{\pi}{2l} \right)^2}{\left[\left(\frac{\pi}{2l} \right)^2 + \left(\frac{n}{R} \right)^2 \right]^2} \right\} \cos \frac{\pi x}{2l} \cos \frac{ny}{R}$$

$$- \frac{q_1^2 l^2}{32} \left(\frac{R\pi}{2nl} \right)^2 \cos \frac{2ny}{R} - \left(\frac{l}{2\pi} \right)^2 \left[\frac{4q_2 l}{R} + \frac{q_1^2}{2} \left(\frac{nl}{R} \right)^2 \right] \cos \frac{\pi x}{l}$$

$$- 2q_1 q_2 \left\{ \frac{\left(\frac{n\pi}{2R} \right)^2}{\left[\left(\frac{3\pi}{2l} \right)^2 + \left(\frac{n}{R} \right)^2 \right]^2} \right\} \cos \frac{3\pi x}{2l} \cos \frac{ny}{R} - 2q_1 q_3 \left\{ \frac{\left(\frac{n\pi}{2R} \right)^2}{\left[\left(\frac{\pi}{2l} \right)^2 + \left(\frac{3n}{R} \right)^2 \right]^2} \right\}$$

$$\times \cos \frac{\pi x}{2l} \cos \frac{3ny}{R} - 16q_2 q_3 \left\{ \frac{\left(\frac{n\pi}{2R} \right)^2}{\left[\left(\frac{\pi}{l} \right)^2 + \left(\frac{2n}{R} \right)^2 \right]^2} \right\} \cos \frac{\pi x}{l} \cos \frac{2ny}{R}. \quad (27)$$

Substituting eqns (26) and (27) into eqn (25) then gives the potential function,

$$V = \frac{1}{2} V_{11}^0 q_1^2 + \frac{1}{2} V_{22}^0 q_2^2 + \frac{1}{2} V_{33}^0 q_3^2 - \Lambda (q_1^2 + 8q_3^2) + \frac{1}{2} V_{112}^0 q_1^2 q_2 + \frac{1}{2} V_{113}^0 q_1^2 q_3 \\ + \frac{1}{24} V_{1111}^0 q_1^4 + \frac{1}{4} V_{1122}^0 q_1^2 q_2^2 + \frac{1}{4} V_{1133}^0 q_1^2 q_3^2 + \frac{1}{4} V_{2233}^0 q_2^2 q_3^2 + \frac{1}{2} V_{1123}^0 q_1^2 q_2 q_3. \quad (28)$$

This is a Taylor expansion about the unloaded equilibrium state, represented by superscript 0, the coefficients being given by,

$$V_{11}^0 = \frac{l^2}{\pi^2 R^2} \frac{8}{(1+\beta^2)^2} + \frac{\pi^2 l^2}{12(1-\nu^2)l^2} \frac{(1+\beta^2)^2}{2}, \quad V_{22}^0 = 16 \left(\frac{l^2}{\pi^2 R^2} + \frac{\pi^2 l^2}{12l^2(1-\nu^2)} \right), \\ V_{33}^0 = \frac{4\pi^2 l^2 \beta^4}{3l^2(1-\nu^2)}, \quad V_{112}^0 = \beta^2 \left(\frac{8}{(1+\beta^2)^2} + 1 \right) \frac{l}{R}, \quad V_{113}^0 = \frac{8\beta^2}{(1+\beta^2)^2} \frac{l}{R}, \\ V_{1111}^0 = \frac{3\pi^2(1+\beta^4)}{16}, \quad V_{1122}^0 = 4\pi^2 \beta^4 \left(\frac{1}{(1+\beta^2)^2} + \frac{1}{(9+\beta^2)^2} \right), \\ V_{1133}^0 = 4\pi^2 \beta^4 \left(\frac{1}{(1+\beta^2)^2} + \frac{1}{(1+9\beta^2)^2} \right), \quad V_{2233}^0 = \frac{16\pi^2 \beta^4}{(1+\beta^2)^2}, \quad V_{1123}^0 = \frac{4\pi^2 \beta^4}{(1+\beta^2)^2}. \quad (29)$$

Here for simplicity we have factored out a common multiplier, as well as introducing the wavelength parameter β , defined as the ratio of the axial to the circumferential wavelength of the q_1 mode,

$$\beta = \frac{2ln}{\pi R}. \quad (30)$$

Differentiating with respect to the modal amplitudes q_i and setting the results to zero then gives the three equilibrium equations,

$$\left(V_{11}^0 - 2\Lambda + V_{112}^0 q_2 + V_{113}^0 q_3 + \frac{1}{6} V_{1111}^0 q_1^2 + \frac{1}{2} V_{1122}^0 q_2^2 + \frac{1}{2} V_{1133}^0 q_3^2 + V_{1123}^0 q_2 q_3 \right) q_1 = 0, \\ (V_{22}^0 - 16\Lambda) q_2 + \frac{1}{2} V_{112}^0 q_1^2 + \frac{1}{2} V_{1122}^0 q_1^2 q_2 + \frac{1}{2} V_{2233}^0 q_2^2 q_3 + \frac{1}{2} V_{1123}^0 q_1^2 q_3 = 0, \quad (31) \\ V_{33}^0 q_3 + \frac{1}{2} V_{113}^0 q_1^2 + \frac{1}{2} V_{1133}^0 q_1^2 q_3 + \frac{1}{2} V_{2233}^0 q_2^2 q_3 + \frac{1}{2} V_{1123}^0 q_1^2 q_2 = 0.$$

We see that $q_1 = 0$ is a valid solution, and bifurcation into q_2 alone is thus possible. Also, the absence of a load term (involving Λ) in the third equation indicates that there is no critical load associated with q_3 alone, as expected. We can treat the amplitude of q_2 as known, and solve eqn (31) for the remaining three variables q_1 , q_3 and Λ . Of these, the final equation can immediately be written,

$$q_3 = - \frac{q_1^2 (V_{113}^0 + V_{1123}^0 q_2)}{2V_{33}^0 + V_{1133}^0 q_1^2 + V_{2233}^0 q_2^2}, \quad (32)$$

giving q_3 directly in terms of q_1 , a consequence of the lack of a load term. The first two equations then can be written in terms of just q_1 and Λ , both linear in Λ . These reduce simply to a cubic equation in q_1^2 which can be solved in closed form. Results directly plotted by computer are presented in Section 6.

5. FULL EQUATIONS

The success of the stress function approach is entirely due to the simplified Donnell equations (3), which allow the linearity in Φ . Under the full formulation extra nonlinearities in u and v block this manoeuvre, and we must return to the initial expansions of eqn (1). The general theory of elastic stability[2, 24, 25] predicts that the extra quartic terms in u and v will affect some of the coefficients of (29) for example. This means that the Donnell equations are accurate as far as cubics[6, 12], but at the quartic level, important for the restabilization of the post-buckling path, they seem to require refinement. An algorithmic form of the general theory[24] has recently been written for microcomputers, as described below, and this presents an ideal opportunity to quantify the effect more completely than earlier[29].

The algorithm involves a general suite of programs written in Pascal, which determine the complete potential function up to quartic level, from any input w function and from any defined set of strain-displacement relations. It is specifically written for microcomputers, in that energy terms and all other variables are stored simply as integer numbers, systematically codified so that all information is efficiently retained. This has the advantage of complete accuracy (within the confines of the initial assumptions), with no round-off error. Algebraic manipulation procedures are developed to determine appropriate u and v functions, perform the required differentiations, multiplications, additions, and integrations, and store, decode and output the resulting list of terms. The process is directly applicable to the general cylindrical shell, and can be used, for example, to find coefficients (29), for the full as opposed to the Donnell formulation. This involves using a second series of routines, which now concentrates on a particular shell geometry, transforming energy terms to real double precision numbers and eliminating the u and v contributions as passive coordinates according to the general scheme[24]; here terms which give a slight nonlinearity to the fundamental path, arising from the unusual strain definition, are ignored. The full suite of programs is being developed with a view to commercial exploitation; it provides basic modal information accurately and cheaply, for a wide range of structural types and formulations.

6. RESULTS AND DISCUSSION

Figure 4 shows some typical results, obtained in this case from the Donnell equations and just two modes, q_1 and q_2 of eqn (1). Although the final form is liable to contamination from other modes, this looping pattern of paths is found with regular consistency in both this and other mode interaction problems[18–21]; we note that it also has been revealed in the cylinder problem by application of the Lindstedt continuum perturbation technique[30]. It is closely tied to the symmetry properties described above[18], is topologically quite robust[19], and seems to typify two-mode interaction in much the same way as the pitchfork form typifies distinct symmetric bifurcation.

The two comparative plots of Fig. 4, obtained for different values of β , the ratio of axial to circumferential wavelength, exhibit some interesting features. $\beta = 1$ is the well-known interaction involving two Koiter circle modes, q_1 at the top and q_2 at the extreme right-hand end (see Fig. 2); $\beta = 1.4$ involves another Koiter circle mode, in a less familiar interaction with its associated q_2 , the latter having a critical load of about 1.5 times P^{KC} , the Koiter circle load. It is apparent that the destabilization is stronger in this second case, even though the critical loads are well separated. It is thus clear that for the axially-loaded cylinder, unlike most buckling problems[2, 25], one cannot rely on remoteness of a potentially-interacting mode on the fundamental path as insurance against severe destabilizing effects.

This point is reinforced in the plots of Fig. 5, in which the "rosette" mode q_3 is included so the results correspond to the potential function of eqns (28) and (29). We remember that q_3 is effectively inextensional with an infinite critical load, and yet for purely geometric symmetry-breaking reasons its inclusion has a considerable destabilizing effect on the response. Results are plotted here for $\beta = 1.2$, equally distinctive contaminating effects being obtained for interactions with other β values. We see that the topology of the looping

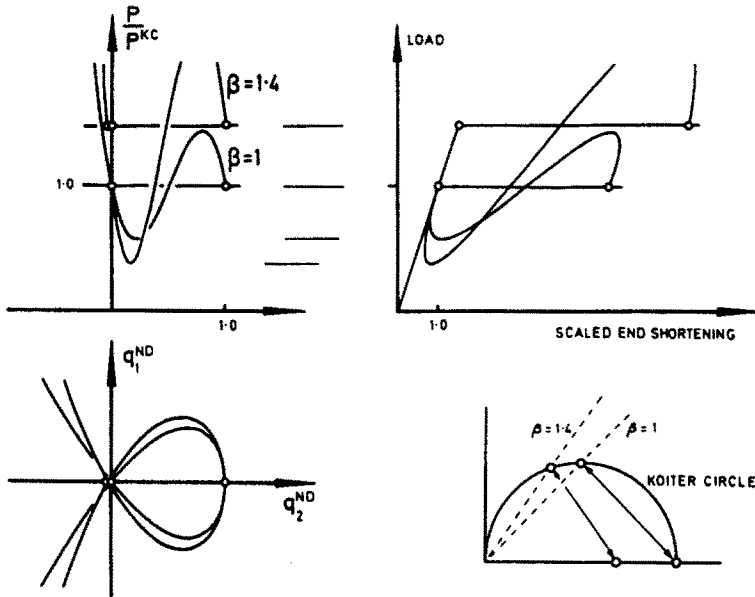


Fig. 4. Non-dimensionalized load/deflection and load/end-shortening plots for two different two-mode interactions, together with relative positions in the wavelength-related space of the Koiter circle.

form is retained, and the destabilization has intensified; with the addition of q_3 , the post-buckling path is pulled closer to the fundamental path on the load/end-shortening plot. Again critical loads on the fundamental path are seen to carry little significance; here both modes lie well off the Koiter circle, with critical loads of about 1.3 and 1.7 times P^{KC} , yet the effective destabilization is certainly as profound as in the examples of Fig. 4. An appropriate symmetry-breaking imperfection, in purest form a combination of q_1 , q_2 and q_3 shapes, would fully round-off the response and give a limit point at a load well below any of the critical values.

We note that if q_3 is to be included, it must be as an active rather than a passive coordinate. Although its critical load is infinite, eliminating it as a passive is only valid over

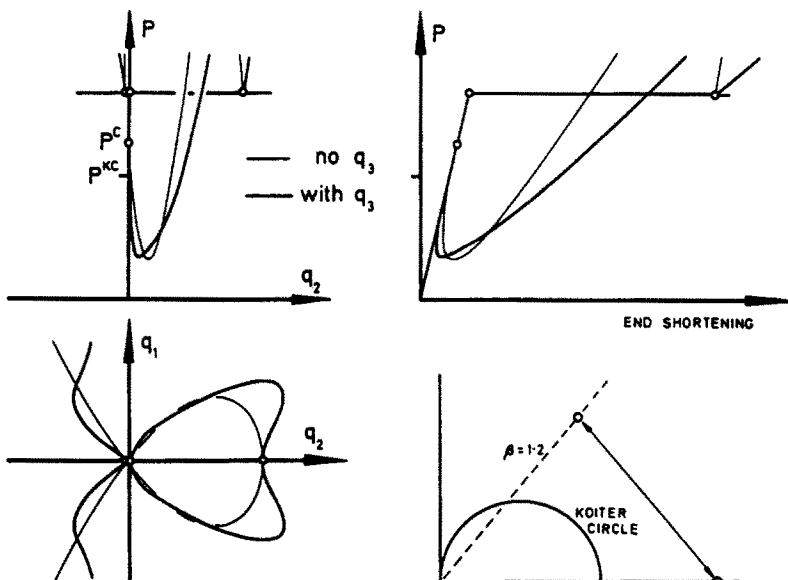


Fig. 5. The effect of adding q_3 to a typical q_1 and q_2 interaction.

a very small post-buckling range, as demonstrated by Williams[26]. This is because the elimination scheme takes quartics associated with a passive mode to be less important than cubics, and in so doing loses the restabilization at the quartic level but retains destabilizing symmetry-breaking effects. It is thus clear that Rayleigh–Ritz modelling with a limited number of modes will give a better overall picture than an attempt to include a large number of (passive) modes in w .

Comparison between Donnell and full formulations can be seen in Table 1, which juxtaposes the two sets of coefficients for potential function (28) at three representative β values. We note that the Donnell potential is complete at this level, but the full formulation will have higher-order terms; no attempt has been made to evaluate these. Plotted results for $\beta = 1$ over the range of practical interest (deflections of the order of the shell thickness) reveal barely discernible differences, so we conclude that, for modes of about equal wavelengths axially and circumferentially, the Donnell strain–displacement equations are adequate. However as β increases the two sets compare less favourably and the Donnell results become more suspect; and we note that an axially-long mode has been suggested by Croll[11] as the possible trigger for the instability. The full algorithm thus provides a reliable means of checking the post-buckling response for such modes. We note finally that the full equations suggest a small but negative curvature to the uncoupled (axially-symmetric) post-buckling path ($V_{2222}^C \neq 0$).

7. CONCLUDING REMARKS

Historically, the study of the buckling of long elastic cylinders has been fraught with difficulty. Classical eigenvalue analysis being thoroughly unreliable, attention switched to imperfection-sensitivity, and to the search for minimum post-buckling loads. Neither approach has been entirely satisfactory.

The problem, as we have seen, is marked by a profound symmetry-breaking interaction and destabilization, followed by almost immediate restabilization as the system picks up the inherent stiffness of a Yoshimura pattern or something like it. It is not enough analytically to select the mode or modes with minimum critical load on the fundamental path, and specifically seek associated interactions[1]. Imperfections round off the sharp corners of Figs 4 and 5 to such an extent that linear eigenvalue results on the fundamental path are barely relevant. It is necessary somehow to select the appropriate buckling form from a number of competing candidates, which may not themselves interact in any way, somewhere on a rapidly descending post-buckling path, finitely far from both the initial critical point

Table 1. Comparison of potential energy coefficients for Donnell and full strain displacement equations, for fixed R/t ratio ($R/t = 121.1$)

	$\beta=1, 1/R=0.1570$		$\beta=5, 1/R=0.7854$		$\beta=25, 1/R=3.927$	
	Donnell	Full	Donnell	Full	Donnell	Full
v_{11}^0	1.000 E-2	1.000 E-2	3.454 E-2	3.415 E-2	7.837 E-1	7.759 E-1
v_{22}^0	8.000 E-2	7.930 E-2	1.000 E 0	9.902 E-1	2.500 E 1	2.475 E 1
v_{33}^0	4.000 E-2	3.969 E-2	1.000 E 0	9.886 E-1	2.500 E 1	2.749 E 1
v_{112}^0	4.712 E-1	4.635 E-1	1.987 E 1	1.924 E 1	2.454 E 3	2.382 E 3
v_{113}^0	3.141 E-1	3.098 E-1	2.323 E-1	2.280 E-1	5.010 E-2	4.931 E-2
v_{1111}^0	3.701 E 0	3.550 E 0	1.158 E 3	1.099 E 3	7.229 E 5	6.874 E 5
v_{1122}^0	1.026 E 1	1.010 E 1	5.784 E 1	2.466 E 1	7.772 E 1	-1.886 E 4
v_{1123}^0	9.870 E 0	9.632 E 0	3.650 E 1	1.065 E 1	3.935 E 1	1.402 E 4
v_{1133}^0	1.026 E 1	9.997 E 0	3.698 E 1	3.572 E 1	3.984 E 1	3.857 E 1
v_{2233}^0	3.948 E 1	3.874 E 1	1.460 E 2	-1.043 E 2	1.574 E 2	-1.522 E 5
v_{2222}^0	0.000 E 0	-1.102 E-2	0.000 E 0	-7.791 E 0	0.000 E 0	-4.294 E 3

and the restabilization marked by the minimum post-buckling load. The minimum load is known to be an unreliable guide and the present scheme supports the known conclusion [10], that it drops to zero as thickness approaches zero.

The study of imperfection-sensitivity must also have been affected by the fact that, analytically, imperfections are almost always taken as harmonic in form, while they are in fact more likely to be dimples. It is possible always to extract a harmonic Fourier component out of a dimple, but this seems rather artificial. An alternative approach is at present actively being pursued, in which the role of a single harmonic function is taken by a combination of functions raised to some power. This can model a dimple quite accurately, and the development of the potential function falls directly into line with our general procedures. Preliminary results have been most encouraging.

Acknowledgements—The authors would like to acknowledge the financial aid of the Science and Engineering Council of Great Britain.

REFERENCES

1. C. R. Calladine, *Theory of Shell Structures*. Cambridge University Press, Cambridge (1983).
2. J. M. T. Thompson and G. W. Hunt, *Elastic Instability Phenomena*. Wiley, Chichester (1984).
3. G. W. Hunt and K. A. J. Williams, On truncation of the structural potential function. *Math. Proc. Camb. Phil. Soc.* **95**, 495 (1984).
4. L. H. Donnell, A new theory for the buckling of thin cylinders under axial compression and bending. *Trans. ASME Aero. Engng AER-56-12*, 795 (1934).
5. T. H. von Kármán and H. S. Tsien, The buckling of thin cylindrical shells under axial compression. *J. aeronaut. Sci.* **8**, 303 (1941).
6. W. T. Koiter, On the stability of elastic equilibrium. Dissertation, Delft, The Netherlands (1945). (English translation: *NASA tech. Transl. F10*, 833 (1967).)
7. R. Thom, *Structural Stability and Morphogenesis* (trans. from French by D. H. Fowler). Benjamin, Reading (1975).
8. J. Kempner, Postbuckling behavior of axially compressed cylindrical shells. *J. aeronaut. Sci.* **21**, 329 (1954).
9. B. O. Almroth, Postbuckling behaviour of axially compressed circular cylinders. *A.I.A.A. J.* **1**, 630 (1963).
10. N. J. Hoff, W. A. Masden and J. Mayers, Post-buckling equilibrium of axially compressed circular cylindrical shells. *A.I.A.A. J.* **4**, 126 (1966).
11. J. G. A. Croll, Lower-bound elasto-plastic buckling of cylinders. *Proc. Inst. Civil Engrs*, Part 2, **71**, 235 (1981).
12. W. T. Koiter, The effect of axisymmetric imperfections on the buckling of cylindrical shells under axial compression. *Proc. K. ned. Akad. Wet.*, Series B **66**, 265 (1963).
13. J. S. Hansen, Influence of general imperfections in axially loaded cylindrical shells. *Int. J. Solids Structures* **11**, 1223 (1975).
14. I. Elishakoff and J. Arbocz, Reliability of axially compressed cylindrical shells with random axisymmetric imperfections. *Int. J. Solids Structures* **18**, 563 (1982).
15. S. Sridharan, A. C. Walker and A. Andronicou, Local plastic collapse of ring-stiffened cylinders. *Proc. Inst. Civil Engrs*, Part 2 **71**, 341 (1981).
16. J. E. Harding, Ring-stiffened cylinders under axial and external pressure loading. *Proc. Inst. Civil Engrs*, Part 2 **71**, 863 (1981).
17. J. M. T. Thompson and G. W. Hunt (Editors), *COLLAPSE: The Buckling of Structures in Theory and Practice*. Proc. IUTAM Symp., University College London, August 1982. Cambridge University Press, Cambridge (1983).
18. G. W. Hunt, Hidden (a)symmetries of elastic and plastic bifurcation. *Appl. Mech. Rev.* **39** (8), 1165 (1986).
19. M. Golubitsky, J. Marsden and D. Schaeffer, Bifurcation problems with hidden symmetries. In *Partial Differential Equations and Dynamical Systems* (Edited by W. Fitzgibbon). Pitman, London (1984).
20. G. W. Hunt and B. A. Burgan, Hidden asymmetries in the Shanley model. *J. Mech. Phys. Solids* **33**, 83 (1985).
21. G. W. Hunt and K. A. J. Williams, Closed-form and asymptotic solutions for an interactive buckling model. *J. Mech. Phys. Solids* **32**, 101 (1984).
22. L. H. Donnell, *Beams, Plates, and Shells*. McGraw-Hill, New York (1976).
23. S. P. Timoshenko and J. M. Gere, *Theory of Elastic Stability*. McGraw-Hill, New York (1961).
24. G. W. Hunt, An algorithm for the nonlinear analysis of compound branching. *Phil. Trans. R. Soc., Lond.* **A300**, 443 (1981).
25. J. M. T. Thompson and G. W. Hunt, *A General Theory of Elastic Stability*. Wiley, London (1973).
26. K. A. J. Williams, Determinacy and mode interaction in elastic systems. Ph.D. thesis, Imperial College, London (1984).
27. D. H. Sattinger, Spontaneous symmetry breaking in nonlinear problems. In *Bifurcation Theory and Applications in Scientific Disciplines* (Edited by O. Gurel and O. E. Rossler). *Ann. N.Y. Acad. Sci.* **316**, 49 (1979).
28. W. F. Thielemann, New developments in the nonlinear theories of the buckling of thin cylindrical shells. *Proc. Durand Centennial Conf.* (Edited by N. J. Hoff and W. G. Vincenti), p. 76. Pergamon, New York (1960).
29. D. O. Brush and B. O. Almroth, *Buckling of Bars, Plates, and Shells*. McGraw-Hill, New York (1975).
30. R. G. Cowell, Looping post-buckling paths of an axially loaded elastic cylindrical shell. *Dynamics and Stability of Systems* (to appear).